An application of flexible constraints in Monte Carlo simulations of the isobaric-isothermal ensemble of liquid water and ice Ih with the polarizable and flexible mobile charge densities in harmonic oscillators model

Saint-Martin, Humberto; Hess, Berk; Berendsen, Herman J. C.

Published in:
Journal of Chemical Physics

DOI:
10.1063/1.1747927

An application of flexible constraints in Monte Carlo simulations of the isobaric–isothermal ensemble of liquid water and ice Ih with the polarizable and flexible mobile charge densities in harmonic oscillators model

Humberto Saint-Martin, Berk Hess, and Herman J. C. Berendsen

Citation: J. Chem. Phys. **120**, 11133 (2004); doi: 10.1063/1.1747927
View online: https://doi.org/10.1063/1.1747927
View Table of Contents: http://aip.scitation.org/toc/jcp/120/23
Published by the American Institute of Physics

An application of flexible constraints in Monte Carlo simulations of the isobaric–isothermal ensemble of liquid water and ice Ih with the polarizable and flexible mobile charge densities in harmonic oscillators model

Humberto Saint-Martin[a)]
Department of Biophysical Chemistry, Rijksuniversiteit Groningen, Nijenborgh 4, 9747 AG Groningen, The Netherlands

Berk Hess
Department of Applied Physics, Rijksuniversiteit Groningen, Nijenborgh 4, 9747 AG Groningen, The Netherlands

Herman J. C. Berendsen
Department of Biophysical Chemistry, Rijksuniversiteit Groningen, Nijenborgh 4, 9747 AG Groningen, The Netherlands

(Received 12 August 2003; accepted 24 March 2004)

The method of flexible constraints was implemented in a Monte Carlo code to perform numerical simulations of liquid water and ice Ih in the constant number of molecules, volume, and temperature and constant pressure, instead of volume ensembles, using the polarizable and flexible mobile charge densities in harmonic oscillators (MCDHO) model. The structural and energetic results for the liquid at $T=298$ K and $\rho=997\ \mathrm{kg\,m^{-3}}$ were in good agreement with those obtained from molecular dynamics. The density obtained at $P=1$ atm with flexible constraints, $\rho=1008\ \mathrm{kg\,m^{-3}}$, was slightly lower than with the classical sampling of the intramolecular vibrations, $\rho=1010\ \mathrm{kg\,m^{-3}}$. The comparison of the structures and energies found for water hexamers and for ice Ih with six standard empirical models to those obtained with MCDHO, show this latter to perform better in describing water far from ambient conditions: the MCDHO minimum lattice energy, density, and lattice constants were in good agreement with experiment. The average $\angle$HOH of the water molecule in ice was predicted to be slightly larger than in the liquid, yet 1.2% smaller than the experimental value. © *2004 American Institute of Physics.* [DOI: 10.1063/1.1747927]

I. INTRODUCTION

The extended range of fields that require a deep understanding of the behavior of water based on molecular detail has led to intensive research by numerical methods, with a variety of potentials to model intermolecular interactions (see e.g., Ref. 1 and references therein). Though in many cases of interest water is either far from ambient conditions, or under narrow confinement, the most used models are still those whose parameters were fitted to reproduce various properties of the liquid under ambient conditions: SPC,[2] SPC/E,[3] TIP3P,[4] and TIP4P.[4] These four models were intended to be used for simulations of biomolecules under ''physiological'' conditions, for example, T ranging from 290 to 320 K, and $P=1$ atm, thus their parameters were tuned to reproduce the experimental density and vaporization enthalpy of liquid water. The compromise between simplicity and accuracy has proven useful and rather difficult to improve,[5] so that the reproduction of the temperature of maximum density could only be attained by adding another interaction site to the model.[6] These models all fail to reproduce the properties of gas-phase water (steam) and the properties of solid-phase water (ices). The search for models that can ensure the reproduction of water properties over a large range of thermodynamic conditions has been directed towards the inclusion of polarizability and flexibility (see Table I of Ref. 1), and to the study of classical trajectories of the nuclei, subject to an approximate quantum force field computed ''on-the-fly.'' [7,8] However, in spite of the large number of existing polarizable and flexible models, none of them has shown as yet any advantage over simple models that is significant enough to encourage its systematic use. An important issue is, of course, computational cost.

Though the inclusion of intramolecular flexibility in analytical model potentials for water was considered since several years ago,[9–15] the difficulties of dealing with quantum degrees of freedom in classical simulations[16] has limited the use of flexible models. A useful, though computationally expensive approach, is the treatment with a path integral formulation,[17,18] following classical trajectories of quasiparticles involved in those degrees of freedom,[19–22] that has already been applied in studies of liquid water.[23–28] A promising alternative with an average effective Feynman–Hibbs potential has also been used,[29] but the approximation breaks down for the high-frequency intramolecular vibrations. To

a)Author to whom correspondence should be addressed. On leave from Centro de Ciencias Físicas, Universidad Nacional Autónoma de México, Apartado Postal 48-3, 62251 Cuernavaca, Morelos, México. Electronic mail: humberto@fis.unam.mx

decouple these latter from classical simulations, a less expensive method of flexible constraints[30,31] has recently been developed[32] that allowed the simulation of a fairly large system (1000 molecules) by means of molecular dynamics, with the polarizable and flexible *ab initio* based mobile charge densities in harmonics oscillators (MCDHO) model.[33] The thermodynamical correctness of the method led to structural and energetic results in agreement with those obtained from the original, fully flexible simulation,[33] considering the loss of the thermal motion in the constrained degrees of freedom. Contrary to the static behavior, the use of flexible constraints had a small, albeit non-negligible effect on the dynamics of the system.[32] Thus, the use of more complex models with new methods of simulation requires that the effects on the results of both models and methods are tested systematically. It is therefore convenient to implement flexible constraints in a Monte Carlo code as this provides another, different approach to simulations, and allows us to perform other tests, such as the effect of flexible constraints on the density of the system, and the search of local minimum energy structures, subject to specific temperatures and pressures.

The sampling of the number of molecules, constant pressure, and temperature (NPT) ensemble can be implemented in the Monte Carlo method rather straightforwardly,[34,35] with exact temperature and pressure controls[36] and without introducing fictitious masses[37,38] or coupling parameters.[39] This ease becomes important when testing other effects, as is the case for a novel model potential and a novel method to include intramolecular flexibility. Thus, in this work flexible constraints were implemented in Monte Carlo simulations, and used to test the ability of the MCDHO[33] model for water to reproduce the density and the energetic and structural parameters of liquid water and ice Ih. Because the MCDHO model was not fitted to reproduce the experimental data of the liquid under ambient conditions, but to the ''correct'' *ab initio* interaction, it should perform better than the standard empirical models in describing ''far-from-ambient-conditions'' water. To evaluate its possible advantages, a comparison was made to the results obtained for water hexamers and for ice Ih with the potentials SPC,[2] SPC/E,[3] SPC/L,[5] TIP3P,[4] TIP4P,[4] and TIP5P.[6]

Moreover, to be able to evaluate the effects of molecular geometry and polarizability, further simulations of ice Ih were performed with the same MCDHO parameters and functional expressions, but constraining the geometry to the average found in the liquid under ambient conditions and to the average found in ice Ih at $T=0.15$ K, and constraining the dipole moment to the average in the liquid, $\mu=2.96$ D, and to the average in ice Ih, $\mu=3.25$ D.

II. THE METHOD

A. Flexible constraints

The method of flexible constraints is based on a Hamiltonian formulation of the dynamics of the system, and was originally developed for molecular dynamics simulations,[32] using the distance between two particles a and b

$$q=\|\mathbf{r}_a-\mathbf{r}_b\|, \tag{1}$$

with position vectors $\mathbf{r}_a$, $\mathbf{r}_b$, velocities $\mathbf{v}_a$ and $\mathbf{v}_b$, and a reduced mass

$$\mu=\frac{m_a m_b}{m_a+m_b}, \tag{2}$$

where the equation of the constraint results in a cancellation of the total potential force $\mathbf{f}(\mathbf{r})=-\nabla V(\mathbf{r})$ and the centrifugal force, both working on the direction of the constraint

$$-\mu q\omega^2-\mathbf{f}(\mathbf{r})\cdot\frac{\partial\mathbf{r}}{\partial q}=0, \tag{3}$$

where $\omega=\|\mathbf{v}_a-\mathbf{v}_b\|/q$ is the corresponding angular velocity. The method can be readily extended to n constraints.

The method of flexible constraints is well suited for molecular dynamics simulations, where all the relevant quantities—positions, velocities, and forces—are computed at each step.

B. Flexible constraints in Monte Carlo simulations

On the other hand, the usual Metropolis[40,41] algorithm for Monte Carlo simulations deals with a random sampling of the configurational space of the system, biased towards the important states by means of a Boltzmann weighting factor. Because the velocities and forces are not computed, a different approach to flexible constraints is required: the condition to keep a thermodynamically correct description is that the high-frequency, quantum degrees of freedom are continuously in their respective ground states, and adjust adiabatically to the change in classical coordinates. This is equivalent to treating the quantum degrees of freedom in the Born–Oppenheimer approximation, usually assumed to be valid for the electronic degrees of freedom. That is, for each Monte Carlo step, the corresponding classical generalized coordinate q_i has to be taken to the value that minimizes its contribution to the total potential energy of the system, i.e.,

$$\frac{\partial}{\partial q_i}H(\mathbf{r},\mathbf{v})=\frac{\partial}{\partial q_i}\left(\frac{1}{2}\mu_i q_i^2\omega_i^2+V(\mathbf{r})\right)=0 \tag{4}$$

(see Ref. 32) that leads to Eq. (3). The velocity-dependent term is not correlated with the configurational term and can be separately averaged over the ensemble. This leads to a constant force, due to two rotational degrees of freedom, projected onto the constraint direction, of $2k_BT/q_i$, where k_B is Boltzmann's constant and T the temperature. Under ambient conditions, this force would lead to an average extension of the O–H bond length by 0.12 pm, which is negligible compared to the O–H bond length of 98.2 pm. Therefore it suffices to zeroing the potential forces acting on the directions of the constraints, so that no net translation or rotation of the molecule should result from the process. The decoupling of the various degrees of freedom is already implicit in the algorithm,[42] thus the treatment of the intramolecular vibrations can be readily implemented in the same way as that used for the positions of the mobile charges.[33] This can be accomplished by referring the coordinates of the three atoms to the center of mass and the principal moments of inertia. In this work, a simple algorithm was devised to find the positions of the atoms that zeroed the projections of

all forces along the vectors connecting each pair. The iterative procedure was combined with the optimization of the mobile charges. Unfortunately, this adds to the computational cost of the Monte Carlo (MC) simulation because the computation of the forces is now required. This is in contrast to the case in molecular dynamics (MD), where the forces are already computed at each step and the additional cost of flexible constraints is negligible.[32] Another difference is that in MD the updating of the polarization and the geometry of the molecules is required only once for each time step, whereas in MC it is needed at every trial move, to satisfy the detailed balance condition.[43] Although it has been proven recently that strict detailed balance is unnecessary for a valid sampling,[44] the procedure of updating only the trial molecule[33,45,46] (called *single update*) has been criticized on this ground.[43,47] However, the results obtained from MD for the vapor–liquid coexistence curve[48] for the model TIP4P-FQ[49] are the same as those from MC with a single update.[45]

In spite of not finding any significant difference with the single update scheme applied to TIP4P-FQ, two alternative schemes have been proposed to comply with detailed balance; the adiabatic nuclear and electronic sampling (ANES)[43,50] and the pair approximation for polarization interaction (PAPI).[47,51] In the ANES scheme, a molecule displacement is followed by a series of random electronic moves of randomly selected molecules, and the resulting configuration is treated as a trial configuration. The electronic moves are accepted using a very low temperature to restrict the charges close to the electronic ground state. In the PAPI scheme, the updating of the dipoles is made taking into account the interactions between the displaced molecule and all molecules within the cutoff radius from the new location, as well as the interactions between all molecules which are distant from the old or the new location of the displaced molecule by less than a parameter R_{iter}. It was shown that the PAPI scheme applied to the polarizable model SCPDP,[52] based on point polarizabilities, yielded different results from single update, due to a bias of the sampling.[47]

Because in this work we are using a different model of polarizability, we decided to test the effects of the different schemes on simulations of liquid water under ambient conditions. Thus, MC simulations of the constant number of molecules, volume, and temperature (NVT) ensemble were done on a cubic box with 343 water molecules at a temperature of $T=298.15$ K and a density of $\rho=997\ \mathrm{kg\,m^{-3}}$. Due to the high computational cost of the PAPI scheme, Ewald sums were not used; this is immaterial at this moment, as we are only interested in looking at possible biases on the sampling caused by the different schemes. In one simulation we used the single update (SU); in another one, ANES with a low temperature of the quantum degrees of freedom (electronic and vibrational) $T_{qm}=0.05$ K and a sampling ratio quantum:classical of 10:1. In a third simulation we used the ANES scheme with the same sampling ratio, but fully optimizing the quantum degrees of freedom, thus $T_{qm}=0$ K. The PAPI scheme was used in a fourth simulation, with $R_{\mathrm{iter}}=0.573$ nm as recommended in Ref. 47. The four simulations started from the same initial configuration and were allowed to run until the criterion of convergence derived from the blocking method[53] was met. In Table I we compare the average per-molecule potential energies resulting from each simulation, as well as the relative number of MC steps required to equilibrate the system and the relative computational cost (CPU time), both referred to the single update scheme. In these latter two regards, SU takes ten times longer than PAPI to attain equilibrium whereas its computational cost is 16 times smaller. The largest difference in energy amounts to only $0.2\ \mathrm{kJ\,mol^{-1}}$ between $\mathrm{ANES}_{0.05}$ and PAPI, while between ANES and SU it amounts to $0.1\ \mathrm{kJ\,mol^{-1}}$. To better assess the correctness of the SU and the ANES schemes, a more stringent test is the comparison of the results to those obtained from molecular dynamics, which is done in Sec. III.

TABLE I. Comparison of the results obtained from the Monte Carlo simulations of ambient liquid water with the MCDHO model,[a] using different sampling schemes: single update (SU), adiabatic nuclear and electronic sampling[b] with $T_{qm}=0.05$ K ($\mathrm{ANES}_{0.05}$) and with $T_{qm}=0$ K (ANES_0), and pair approximation for polarization interaction[c] (PAPI). The energy $\langle U\rangle$ is in $\mathrm{kJ\,mol^{-1}}$, NS_{rel} is the relative number of MC steps needed to attain equilibrium, and tc_{rel} is the relative computational cost (CPU time), both referred to the SU scheme.

	SU	$\mathrm{ANES}_{0.05}$	ANES_0	PAPI
$\langle U\rangle$[d]	−51.5	−51.4	−51.5	−51.6
NS_{rel}	1	0.9	0.8	0.1
tc_{rel}	1	3	6	16

[a]See Ref. 33.
[b]See Refs. 43 and 50.
[c]See Refs. 47 and 51.
[d]The statistical uncertainty is $\pm 0.1\ \mathrm{kJ\,mol^{-1}}$ in all cases.

III. TEST CASE: LIQUID WATER UNDER AMBIENT CONDITIONS

Because there already exist data for liquid water with flexible constraints,[32] a direct comparison of the structural and energetic results from Monte Carlo simulations can be readily done: the same three systems of Ref. 32 were studied, that is, NVT ensembles of 1000 MCDHO water molecules in periodic cubic boxes at a fixed density of $997\ \mathrm{kg\,m^{-3}}$ and a fixed temperature of $T=298$ K. The same cutoff of 1 nm was used for the particle–particle interactions, and Ewald sums[54–56] to treat the long-range electrostatic interactions. The correction to the dispersion energy amounts to $-0.3\ \mathrm{kJ\,mol^{-1}}$. The same convention as in Ref. 32 was used to name the simulations: MC–FF (fully flexible), MC–RC (rigidly constrained), and MC–FC (flexibly constrained).

Besides a possible bias in the sampling with the SU scheme, a new problem arises when including the Ewald sums, namely the updating of the corresponding forces for the optimization of the geometry and the polarization of each molecule. This was neglected in the original MCDHO simulations[33] due to the high computational cost. As a result, when we used molecular dynamics to simulate ambient liquid water,[32] including the Ewald forces, we found a small difference in energy of $0.3\ \mathrm{kJ\,mol^{-1}}$. The ANES scheme applied to Monte Carlo simulations circumvents the evaluation of the forces and provides a method to test our previous

TABLE II. Comparison of the results obtained from the MC-FF, MC-FC, and MC-RC simulations with the MCDHO model,[a] to those obtained from molecular dynamics,[b] and to experimental data. The quantum corrections found in Ref. 28 were used to compute the evaporation enthalpies of the models.

Model	$U_g - U_l$ (kJ mol^{-1})	ΔH_{vap} (kJ mol^{-1})	$\langle r_{OH}\rangle$ (pm)	Δr_{OH} (pm)	$\langle r_{HH}\rangle$ (pm)	Δr_{HH} (pm)	$\angle$HOH (degrees)
MD-FF	43.3	⋯	98.5	2.6	153.8	5.3	102.7
MC-FF	43.4	⋯	98.4	2.6	153.7	5.3	102.7
MD-FC	46.9	43.2	98.2	0.9	153.4	1.9	102.7
MC-FC	46.9	43.2	98.2	0.9	153.4	2.0	102.7
MD-RC	46.8	43.1	98.4	⋯	153.7	⋯	102.7
MC-RC	46.9	43.2	98.4	⋯	153.7	⋯	102.7
Experimental	⋯	44.0[c]	96.6[d]	⋯	151.0[d]	⋯	102.8[d]
⋯	⋯	⋯	97.0[e]	⋯	155.0[e]	⋯	106.1[e]

[a]See Ref. 33.
[b]See Ref. 32.
[c]See Ref. 103.
[d]See Ref. 104.
[e]See Ref. 83.

conclusion that the difference in energy was due to the handling of the Ewald sums with the particle-mesh method[57–60] in the molecular dynamics. Thus, the ANES scheme was used, with $T_{qm}=0.05$ K and a sampling ratio quantum:classical of 10:1. The comparison to previous results is presented in Table II. The Monte Carlo (MC) simulations reproduced the energetic and structural results of molecular dynamics, with rather small variations. It is worthwhile to notice that the SU scheme taken from Ref. 33 produced in this case the same difference in energy as previously reported,[32] 0.3 kJ mol^{-1}, and a slightly shorter intramolecular H–H distance, 153.0 pm. Therefore, the reasonable computational cost, the right sampling, and the handling of long-range effects, which does not require the evaluation of forces, makes ANES the method of choice.

Care must also be taken to ensure convergence of the MC sampling,[61,62] so in the subsequent simulations of this work we used the ANES scheme[43,50] for the sampling and the blocking method[53] to assess convergence.

IV. THE DENSITY OF LIQUID WATER

One of the intentions of this work is to find the possible effects that flexible constraints may cause on the prediction of the density of liquid water. Because the convergence of the density is rather slow,[6] a smaller system of 343 MCDHO water molecules was used. Calibration runs of the (NVT) ensemble produced the same energetic and structural results as found with 1000 molecules.

For comparison to a model that was fitted to the experimental density under ambient conditions, the same small system was simulated with 343 TIP5P[6] water molecules. From the (NVT) simulation without Ewald sums, we found the same per-molecule potential energy as reported in Ref. 6, $U_{gas}-U_{liq}=41.3$ kJ mol^{-1}. A comparison of the radial distribution functions obtained from (NVT) simulations of both MCDHO and TIP5P models to experimental data.[63] is shown in Figs. 1–3.

Both models, TIP5P and MCDHO, reproduce the experimentally determined[63] g_{OO} radial distribution function, including the second and third maxima, though MCDHO slightly exaggerates the latter. The g_{OH} and g_{HH} obtained with TIP5P also match quite well those obtained from experiment, whereas MCDHO produces a seemingly more structured liquid: though the locations of the maxima are correct, the heights are overestimated. It has to be remembered, though, that the heights determined from experiment are not as reliable as the positions.[64] However, it has been

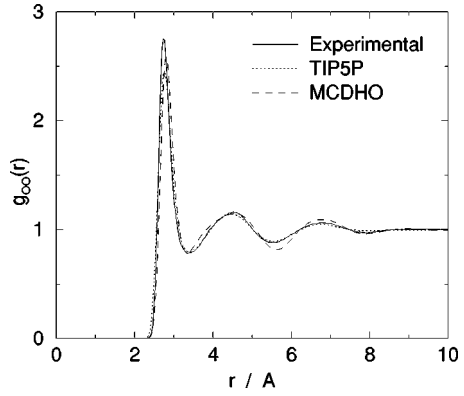

FIG. 1. Comparison to experiment (see Ref. 63) of the OO radial distribution functions obtained from simulations with the models MCDHO (Ref. 33) and TIP5P (Ref. 6).

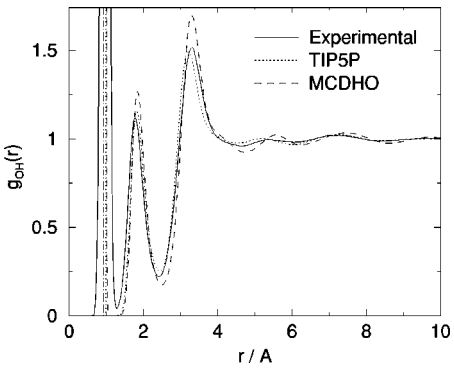

FIG. 2. Comparison to experiment (Ref. 63) of the OH radial distribution functions obtained from simulations with the models MCDHO (Ref. 33) and TIP5P (Ref. 6).

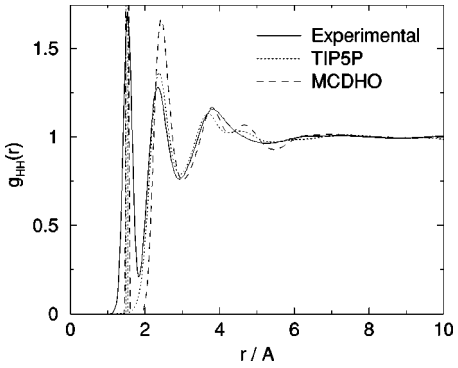

FIG. 3. Comparison to experiment (Ref. 63) of the HH radial distribution functions obtained from simulations with the models MCDHO (Ref. 33) and TIP5P (Ref. 6).

shown[28] that vibrational quantum effects lower the first peak of the g_{OH} obtained with MCDHO. It is worth noticing that an empirical model fitted to the liquid properties includes these quantum effects in an average manner, whereas a model based on single molecule properties and *ab initio* interactions does not.

Further Monte Carlo simulations of the (NPT) ensemble were performed with a computational cell of 343 water molecules at $T=298.15$ K and $P=1$ atm $(=0.101\,325$ MPa). Volume changes were attempted approximately every 1000 configurations, and their magnitude as well as the ranges for molecular rotations and translations were adjusted to yield acceptance rates of $\sim 40\%$. A spherical cutoff radius of 1.085 nm was used and, because TIP5P was fitted in simulations without long-range corrections,[6] Ewald sums and a dispersion correction were applied only for the MCDHO model. The convergence of the results was tested with the blocking method of Flyvbjerg and Petersen.[53] Very large runs of 10^9 MC steps were required to attain a statistically meaningful sample, with a standard error of $e_{\mathrm{rms}}=1\ \mathrm{kg\,m^{-3}}$. The resulting density found with TIP5P was $\rho=1006\ \mathrm{kg\,m^{-3}}$, that is less than 1% higher than previously reported.[6] This slight difference may be due to the longer cutoff radius employed here. The densities predicted with the MCDHO model were $\rho=1010\ \mathrm{kg\,m^{-3}}$ for MC-FF, $\rho=1008\ \mathrm{kg\,m^{-3}}$ for MC-FC, and $\rho=1005\ \mathrm{kg\,m^{-3}}$ for MC-RC. These values show that the effect of the constraints results in an almost negligibly lower density than that obtained with the classical sampling of the intramolecular degrees of freedom. Though small, the effect diminishes the difference with respect to the experimental value, $\rho=997\ \mathrm{kg\,m^{-3}}$. It is worth noticing that quantum corrections should lower the density obtained from numerical simulations.[29]

V. ICE IH

One of the expectations of a flexible and polarizable water model is that it should be able to reproduce the behavior of water under various different thermodynamical conditions. The MCDHO model has been successful in doing that for the gas and the liquid phases,[33] but it has been argued that an accurate potential ought to predict that phases resembling the phases of ice are in local potential minima and have the same energies.[65] Another important point is the comparison of the predictions obtained with a complex model to those obtained with standard, nonpolarizable, rigid, and less expensive water models. Thus, in this section we present the performance of the MCDHO model to simulate ice Ih, and compare the results to the standard models SPC,[2] SPC/E,[3] SPC/L,[5] TIP3P,[4] TIP4P,[4] and TIP5P.[6]

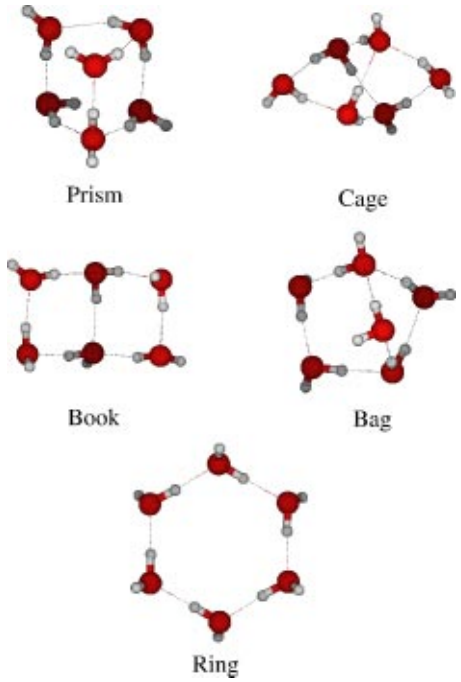

FIG. 4. Lowest energy water hexamers.

A. Water hexamers

Because in this work we make a Monte Carlo search for the phases in local potential energy minima, we decided to test the method by finding the most stable water hexamers with each of the models, as it is known[66] that there are several stable configurations whose energies lie within $8\ \mathrm{kJ\,mol^{-1}}$: prism, cage, book, ring, and bag (Fig. 4).

The stable hexamers found previously[33] with the MCDHO model were used as the starting configurations for each model, changing the intramolecular geometry accordingly. The Monte Carlo procedure was used with a temperature of $T=0.15$ K and small displacement and rotation steps, for an acceptance rate of 95%. No annealing was employed because the aim was to obtain local energy minima, close to the starting structures. The sampling was continued to generate 1000 configurations with energy differences of less than $0.001\ \mathrm{kJ\,mol^{-1}}$, from which the lowest energy was chosen. The interaction energies of the resulting hexamers are presented in Table III.

Several data are worth noticing for the three-site models: (1) all of them are able to produce five different configurations with energies within $8\ \mathrm{kJ\,mol^{-1}}$; (2) all of them yield the book configuration as the global minimum. This result was also obtained by Niesse and Mayne,[67] and by Wales and Hodges[68] with the TIP3P model. (3) None of them maintained the prism configuration, that has the maximum number of hydrogen bonds; instead, all of them lost one and

TABLE III. Total interaction energies (kJ mol^{-1}) obtained with each model for the most stable water hexamers shown in Figs. 4 and 5. The numbers on the second row are the number of hydrogen bonds in each configuration.

Model	Prism 9 HB	Cage 8 HB	Book 7 HB	Ring 6 HB	Bag 7 HB	Wedge 8 HB
SPC	···	−200.0	−203.6	−199.8	−197.5	−198.0
SPC/E[a]	···	−186.3	−190.4	−186.4	−183.7	−184.1
SPC/L	···	−200.7	−202.8	−197.3	−197.4	−198.3
TIP3P	···	−195.3	−199.9	−198.5	−194.4	−195.1
TIP4P	−196.3	−197.7	−192.9	−185.7	−191.3	−194.6
TIP5P	−191.6	−189.6	−195.8	−197.9	−192.9	−188.2
MCDHO[b]	−184.9	−182.8	−184.1	−185.3	−184.1	−181.9
ab initio[c]	−192.0	−191.6	−190.8	−187.4	−184.5	···

[a]For this model a polarization correction (Ref. 3) of 5.22 kJ mol^{-1} per molecule was applied to the energy.
[b]See Ref. 62.
[c]Energies for prism, cage, book and ring configurations from Ref. 70; the energy for the bag configuration from Ref. 66. No *ab initio* value has been reported for the wedge.

evolved to a truncated pyramid (or wedge, Fig. 5) form. (4) All of them produced chair-like ring conformations (Fig. 5), with dihedrals ϕ between 130° and 145°. (5) All of them exaggerate the total interaction energy, as compared to the *ab initio* values, apart from SPC/E, for which the correction of 5.22 kJ mol^{-1} per molecule produces a substantially closer agreement. This correction represents the energetic cost of inducing a larger dipole moment than that of an isolated molecule,[3] and the same effect is built into the MCDHO model.[33]

The cage structure has been recognized as the experimental minimum,[69] whereas the *ab initio* ordering without inclusion of zero-point energy (ZPE) has been proposed as shown in Table III: prism, cage, book, ring, and bag, from lower to higher energy;[70] but other recent calculations with a counterpoise-corrected potential energy surface, yield the ring as the minimum.[71] At any rate, the five isomers lie so close in energy that their relative ordering is rather difficult to assess with certainty. However, the prism structure is among them, and our results show that three-site models fail to reproduce it.

The TIP4P model does yield the prism configuration as having the second lowest energy, and we predict the minimum to be the cage, in agreement with the results of Wales and Hodges.[68] The other lowest energy configurations are, in order of increasing energy, the wedge, the book, the bag and the ring, this latter with a dihedral $\phi=142.3°$. TIP5P and MCDHO produce more planar cyclic structures, with dihedrals $\phi=175.0°$ and $\phi=166.5°$, respectively, that also happen to be the minima in both cases, whereas the highest energies correspond to the cage and the wedge; however TIP5P favors the book and the bag over the prism, opposite to MCDHO.

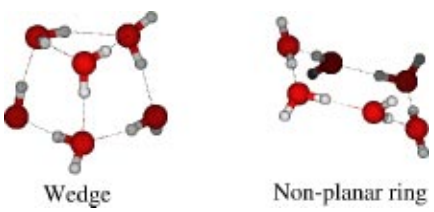

FIG. 5. Wedge and nonplanar cyclic water hexamers.

Though the configurations are asymmetric, the analysis of the average O–O distance predicted with each model (Table IV) will be useful to assess the reliability of the densities of ice Ih that we present in the next subsection.

It can be seen in Table IV that TIP5P produces the most closely packed hexamers, followed by SPC/L, SPC/E, and TIP4P, whereas the average nearest-neighbor O–O distances predicted by SPC and TIP3P are rather similar. MCDHO produces the longest separations. It is to be noted that the six-membered structures to be found in ice Ih are chair-like ring configurations, and all models predicted it to be the most closely packed, with an average O–O distance that is shorter than in the optimal dimer. This result shows the influence of collective effects even for pair-additive models. It also shows that the O–O distances predicted by the models for ice Ih should be shorter than their corresponding optimal dimer.

B. Idealized ice Ih at $T=0.15$ K

The relative simplicity of MCDHO with respect to other polarizable models, allows for a large enough number of molecules in the computational cell that no large deviations from a cubic shape are required. In this work, we used a random starting configuration of 768 water molecules in a hexagonal arrangement and zero total dipole moment generated with the procedure described in Ref. 64, in a rectangular box of lengths 2.6945 nm×3.1113 nm×2.9334 nm, for a density of $\rho=933$ kg m^{-3}. This latter value was estimated from scaling the measured density at 250 K with the corresponding variation of the lattice parameters[72] between 10 and 250 K.

For each model, Monte Carlo simulations of the (NVT) ensemble at $T=0.15$ K were performed with a cutoff radius of 1.058 nm. Though the empirical models were fitted to include the long-range interactions in an average manner, we considered the periodicity of the system to require the use of Ewald sums in all cases. The dispersion energy beyond the cutoff radius was considered to be isotropic, though. This latter contribution is only −0.1 kJ mol^{-1} for the empirical models, and −0.3 kJ mol^{-1} for MCDHO.

After the minimum energy was reached, generally in 10^7 configurations, further Monte Carlo simulations of the (NPT) ensemble at $P=1$ atm were performed, with inde-

TABLE IV. Average O–O distances (pm) obtained with each model for the most stable water dimer (second column) and for the hexamers shown in Figs. 4 and 5.

Model	Dimer	Prism	Cage	Book	Ring	Bag	Wedge
SPC	275.2	⋯	278.0	274.1	271.4	274.6	278.2
SPC/E	273.4	⋯	276.1	272.1	269.6	272.7	276.2
SPC/L	273.1	⋯	275.6	272.0	269.8	272.6	275.8
TIP3P	274.7	⋯	277.6	273.8	270.9	274.3	277.3
TIP4P	275.0	278.6	275.8	273.4	272.1	273.5	276.3
TIP5P	267.6	277.2	274.5	269.0	265.5	269.4	274.3
MCDHO[a]	291.8	289.8	287.1	281.0	272.8	281.0	286.4
ab initio[b]	290.7	284.0	280.7	276.6	270.7	276.9	⋯

[a]See Ref. 62.
[b]See Ref. 105 for the dimer and Ref. 66 for the hexamers.

pendent expansions in the X, Y, and Z directions, to find the predictions of the models for the density, the potential energy, the average O–O distances, and the lattice constants. This procedure constitutes a Monte Carlo search for the (local) lowest energy conformations, and allows the anisotropic geometrical relaxation of the lattice. The results are presented in Table V.

Because perfect ice Ih structures with differently randomized hydrogens give slightly different energies and densities, the use of a few hundred molecules in the minimization limits the accuracy[73] to $\sim 0.1\ \mathrm{kJ\,mol^{-1}}$ and $10\ \mathrm{kg\,m^{-3}}$. Therefore, to propose average O–O distances and lattice constants with an accuracy of 10^{-12} m, we considered the distributions around each molecule, instead of taking only averages of the distances between planes, as is done experimentally.[72] The values presented in Table V were obtained from Gaussian fits to the distributions, and due to the previously discussed limitations, the expected uncertainty is $\sim \pm 1$ pm.

In agreement with previously reported results at various temperatures,[74–78] the densities found with the empirical models are all higher than the experimental value. Moreover, the density we found for TIP4P, $\rho = 977\ \mathrm{kg\,m^{-3}}$, matches a previously reported value,[79] and the density we found with SPC/E, $\rho = 979\ \mathrm{kg\,m^{-3}}$, is consistent with the values reported[78] for temperatures ranging from 150 to 290 K. Though higher densities have been reported by Dong *et al.*[80] for SPC/E, TIP3P, and TIP4P, from the dipoles these authors present, it is not clear that they used the right parameters or the right rigid geometries. At any rate, the highest density was obtained with the TIP5P model, whereas that predicted by the MCDHO model, $\rho = 941\ \mathrm{kg\,m^{-3}}$, is significantly closer to the experimental value than those obtained with the empirical models. To check that this was not an artifact due to the use of Ewald sums, we repeated the Monte Carlo searches without them, and found the same results, within the above mentioned uncertainties (results not shown). The ordering from highest to lowest density is: TIP5P, SPC/L, SPC/E, TIP4P, TIP3P, SPC, and MCDHO, the same that we found previously for the packing of the hexamers.

With regard to the potential energies, the experimental value in Table V includes corrections for intermolecular and intramolecular vibrations.[65] Considering that rigid empirical models include these contributions for the liquid, a correction from a shift in the intramolecular ZPE when going from the liquid to the solid can be estimated from experimental data[81] as $-1.3\ \mathrm{kJ\,mol^{-1}}$. For MCDHO an estimate was made from the change in vibrational intramolecular energy found for the liquid in Ref. 28: $\mathrm{ZPE}_{\mathrm{gas}}^{\mathrm{intra}} - \mathrm{ZPE}_{\mathrm{liquid}}^{\mathrm{intra}} = 2.5\ \mathrm{kJ\,mol^{-1}}$. This value was added to the empirical correction, for a total of $1.2\ \mathrm{kJ\,mol^{-1}}$. Of course, a more accurate estimate should be obtained from path–integral molecular dynamics, but this is beyond the aim of the present study.

TABLE V. Comparison to experimental data of the densities ($\mathrm{kg\,m^{-3}}$), the potential energies $\Delta U = U_{\mathrm{ice}} - U_{\mathrm{gas}}$ ($\mathrm{kJ\,mol^{-1}}$), the average O–O distances (pm), the lattice constants a and c (pm), and the c/a ratio, predicted by various models for ice Ih at $T = 0.15$ K.

Model	ρ	$-\Delta U$[a]	$\langle r_{\mathrm{OO}} \rangle_a$	$\langle r_{\mathrm{OO}} \rangle_c$	a	c	c/a
SPC	960	57.8	273.0	272.4	445.2	725.4	1.629
SPC/E	979	57.5	271.2	270.9	442.3	721.1	1.630
SPC/L	982	58.0	270.8	270.5	442.3	720.1	1.628
TIP3P	963	55.4	273.0	272.4	445.0	725.3	1.630
TIP4P	977	58.3	271.2	270.8	442.7	720.8	1.628
TIP5P	1045	61.4	265.1	264.9	432.7	706.3	1.632
MC-FC	941	60.1	274.7	274.4	448.4	730.8	1.630
Experimental	933[b]	58.8[c]	275.3[d]	274.6[d]	449.7[b]	732.1[b]	1.628[b]

[a]A correction of $-1.3\ \mathrm{kJ\,mol^{-1}}$ to the shift in intramolecular ZPE was used for the empirical models, whereas for MCDHO the correction amounted to $1.2\ \mathrm{kJ\,mol^{-1}}$ (see text).
[b]See Ref. 72. The experimental density was computed from the lattice constants.
[c]See Refs. 65 and 99.
[d]See Ref. 91. Because the oxygen coordination deviates from perfectly tetrahedral ($c/a = 1.628$, instead of 1.633), the nearest neighbor distance is not the same in all directions.

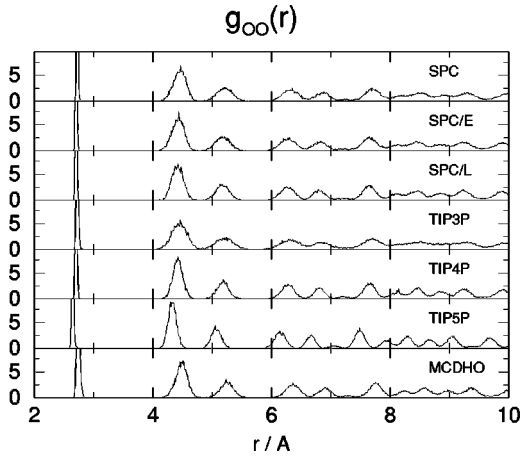

FIG. 6. Comparison between the OO radial distribution functions obtained with the models SPC, SPC/E, SPC/L, TIP3P, TIP4P, TIP5P, and MCDHO.

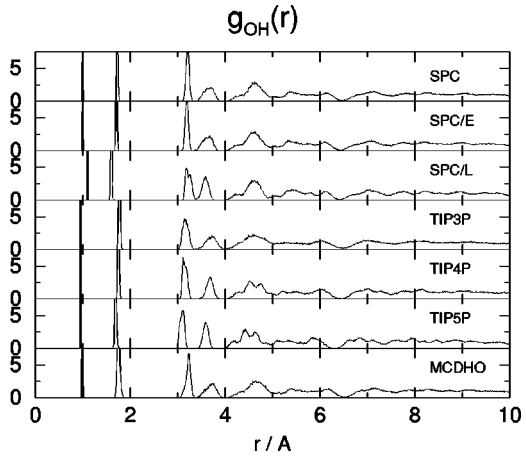

FIG. 7. Comparison between the OH radial distribution functions obtained with the empirical models SPC, SPC/E, SPC/L, TIP3P, TIP4P, TIP5P, and MCDHO. After the dip at a distance corresponding to the lattice constant c, the distribution attains a value of 1.

From Table V it can be seen that the three- and four-site models slightly underestimate the lattice energy, while TIP5P and MCDHO slightly overestimate it. However, the agreement with the experimentally determined value is quite remarkable, as none of them was fitted to the properties of ice. In fact, MCDHO should be expected to perform well in this respect, because it accounts explicitly for nonadditive effects, whereas the empirical models account for them in an average manner. Thus, the good reproduction of the energy of ice suggests that most of the nonadditive effects are already present in liquid water.

Though the O–O distances and lattice constants obtained from the empirical models are shorter than the experimental values, the c/a ratio remains in good agreement with experiment. In the case of MCDHO, the agreement includes all the quantities, showing the ability of the model to account for collective nonadditive effects. This is not the case for the rigid polarizable TIP4P-FQ model,[49] which not only overestimates the density, but produces a large ratio[77] of $c/a = 1.641$. This is an example of a polarizable model with a worse performance than its nonpolarizable counterpart.

The radial distribution functions (RDFs) are shown in Figs. 6, 7, and 8. The RDFs obtained from the empirical models are shifted to the left with respect to those obtained from MCDHO. The $g_{OO}(r)$ corresponds to the crystalline arrangement of the oxygens, whereas the $g_{OH}(r)$ and $g_{HH}(r)$ show that the ordering of the hydrogens is kept only at a rather short range of the order of the size of the unit cell, as shown by the dips at distances corresponding to the lattice constant c for $g_{OH}(r)$, and a for $g_{HH}(r)$. These features are in agreement with previous numerical simulations with the NCC-vib potential.[82]

With regard to the distortion of the water molecule in ice Ih (Table VI), the MCDHO model correctly predicts the elongation of the OH bonds; however, the predicted bond angle, $\angle \mathrm{HOH} = 103.8°$, is smaller than in the gas phase $\angle \mathrm{HOH} = 104.52°$, though larger than the prediction in the liquid $\angle \mathrm{HOH} = 102.7°$. The value determined from a neutron diffraction experiment[83] for the molecule in the liquid is $\angle \mathrm{HOH} = 106.1°$, which is also predicted by quantum mechanical calculations[84,85] and by a simulation with a quantum "on-the-fly" potential.[8] The large value assumed for the water molecule in ice Ih[86,87] from the tetrahedral coordination of the oxygens, $\angle \mathrm{HOH} = 109.47°$, was under debate for some time.[88–90] Nevertheless, the value deduced from a recent analysis of single-crystal neutron diffuse scattering[91] is only $\angle \mathrm{HOH} = 105.1°$, even smaller than the liquid-phase angle. This seems inconsistent, as one would expect that the hydrogen-bond network in ice induces a larger widening of the molecule than in the liquid. Considering that the measurements in solids present less difficulties than those in liquids, the solid-phase angle should be more accurate and the liquid-phase angle should be expected to be smaller or at most equal. Thus, the prediction of the MCDHO model is underestimated by a mere 1%–2%, however qualitatively opposite to the experimentally determined behavior. This should be compared to the prediction of $\angle \mathrm{HOH} = 101.3°$ obtained with the model NCC-vib.[82]

The MCDHO model predicted per-molecule average dipole moment in the liquid is[28,62] $\mu = 2.96$ D, in agreement

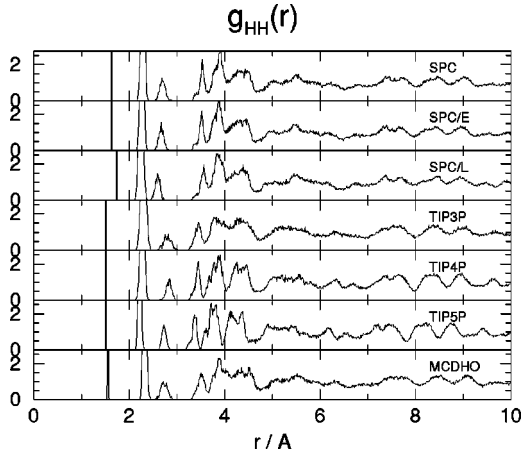

FIG. 8. Comparison between the HH radial distribution functions obtained with the empirical models SPC, SPC/E, SPC/L, TIP3P, TIP4P, TIP5P, and MCDHO. After the dip at a distance corresponding to the lattice constant a, the distribution attains a value of 1.

TABLE VI. Deformation and polarization of the water molecule in ice Ih. Comparison to experiment of MCDHO predicted values.

	$\langle r_{OH}\rangle$ (pm)	Δr_{OH} (pm)	$\langle r_{HH}\rangle$ (pm)	Δr_{HH} (pm)	$\angle$HOH (degrees)	μ (D)	$\Delta\mu$ (D)
MCDHO	99.4	0.3	156.4	0.4	103.8	3.25	0.09
Experimental[a]	99.7	⋯	163.0	⋯	105.1	3.00	⋯

[a]Intramolecular geometry from Ref. 91, experiment at $T=20$ K, and dipole moment from Ref. 99.

with recent experimental[92,93] and theoretical evaluations that show this dipole moment to yield the right dielectric constant.[94] However, the convergence of this latter result has been recently criticized,[95] and there is some theoretical evidence that the polarizability in the liquid phase is up to 9% smaller than in the gas phase.[96–98] Thus, the correct value remains an open question.

The MCDHO result for the molecule in ice Ih is $\mu=3.25$ D, close to that obtained with the NCC-vib model,[82] and to the upper bound derived from the experimental electric permittivities[99] for ice VI, that is partly orientationally ordered. For ice Ih the corresponding experimental evaluation lies between $\mu=2.45$ and 3.00 D. However, the derivation of these values neglects the contributions to the dielectric constant of multipole moments higher than the dipole. Instead, a recent study using an induction model[100] and including moments up to hexadecapole, found the average per-molecule dipole to be $\mu=3.09$ D in ice Ih. Thus, the MCDHO value is overestimated by only 5%. A further consideration to be taken into account is that the induction model includes only electronic polarizability, whereas the simulation with MCDHO also includes the effect of the elongation of the O–H bonds. At any rate, the MCDHO result that the molecular dipole moment in ice Ih, $\mu=3.25$ D, is $\sim$15% higher than in the cyclic hexamer,[33] $\mu=2.80$ D, is in agreement with a recent *ab initio* study.[101]

C. Simulations with simplified models

It has recently been found[62] that simplified versions of MCDHO having the liquid-phase average geometry and dipole moment perform rather well in simulations of liquid water. In this subsection we use the same approach to generate two other simplified versions, both with the average ice Ih geometry and one of them with the average dipole moment. Thus, four simplified versions are used: (1) MC-RC$_l$, that is polarizable and has the liquid geometry, $r_{OH}=98.4$ pm and $\angle$HOH$=102.7°$; (2) MC-RC$_{npl}$, nonpolarizable with the same geometry and a fixed dipole $\mu=2.96$ D; (3) MC-RC$_{Ih}$, polarizable with the ice Ih geometry, $r_{OH}=99.4$ pm and $\angle$HOH$=103.8°$; and (4) MC-RC$_{npIh}$, nonpolarizable with ice Ih geometry and a fixed dipole $\mu=3.25$ D. The results are shown in Table VII.

The two versions with the ice Ih geometry produce virtually the same results as the polarizable and flexible model, in agreement with the conclusion of Ref. 62 that a simplified, rigid, and nonpolarizable model can be reliably used in numerical simulations, provided that the intramolecular geometry and polarization are consistent with the intermolecular interactions. The good performance of the TTM2-R model, which keeps the gas-phase geometry, seems to contradict this conclusion. However, the effects of intramolecular geometry are included in the parameters of this latter model.[79]

The rigid, nonpolarizable MC-RC$_{npl}$ version yields a low density, but the results obtained with the polarizable version with the liquid geometry, MC-RC$_l$, are in excellent agreement with experiment, even better than those of the polarizable and flexible model. This is fortuituous, as the simulations do not include any quantum correction to intermolecular vibrations and librations. Nevertheless, the comparison shows that while the intramolecular geometry does not change significantly from the liquid to the solid, a mere 1% in the elongation of the O–H bonds, but the polarization does: the average per-molecule dipole moment of the MC-RC$_l$ model is $\mu=3.21$ D, that is 1% lower than MC-FC,

TABLE VII. Comparison to experimental data of the densities (kg m^{-3}), the potential energies $\Delta U=U_{ice}-U_{gas}$ (kJ mol^{-1}), the average O–O distances (pm), the lattice constants a and c (pm), and the c/a ratio, predicted for ice Ih at $T=0.15$ K by rigid and nonpolarizable models derived from MCDHO, and by the *ab initio* model TTM2-R.[a]

Model	ρ	$-\Delta U$[b]	$\langle r_{OO}\rangle_a$	$\langle r_{OO}\rangle_c$	a	c	c/a
MC-FC	941	60.1	274.7	274.4	448.4	730.8	1.630
MC-RC$_l$	931	59.9	275.7	275.4	450.0	733.6	1.630
MC-RC$_{npl}$	902	58.9	278.6	278.4	454.8	740.8	1.629
MC-RC$_{Ih}$	941	60.1	274.8	274.5	448.0	731.3	1.632
MC-RC$_{npIh}$	942	60.1	274.8	274.4	448.1	730.7	1.630
TTM2-R	942	61.5	⋯	⋯	447.8	731.3	1.633
Experimental	933[c]	58.8[d]	275.3[e]	274.6[e]	449.7[c]	732.1[c]	1.628[c]

[a]See Ref. 79.

[b]For the MCDHO-derived models a correction was applied to the energy, with an estimate of the change in intramolecular zero-point energy of 1.2 kJ mol^{-1} (see text).

[c]See Ref. 72. The experimental density was computed from the lattice constants.

[d]See Refs. 65 and 99.

[e]See Ref. 91. Because the oxygen coordination deviates from perfectly tetrahedral ($c/a=1.628$, instead of 1.633), the nearest neighbor distance is not the same in all directions.

but 8% higher than the liquid phase value, $\mu = 2.96$ D. As stated in the previous subsection, the actual value of the permolecule dipole moment in condensed phases is not yet well established; but our results show that the high values we obtain are consistent with a good description of the energetics and structure of condensed phases.

VI. DISCUSSION

In this work we showed how to implement flexible constraints in numerical simulations with the Monte Carlo method, and obtained results in agreement with previous simulations with molecular dynamics. We then used the method with the flexible and polarizable MCDHO model to compute the density of liquid water under ambient conditions, where we found only rather small differences among the results of simulations with versions of the model that were fully flexible, flexibly constrained, and rigidly constrained.

Opposite to many other polarizable models, MCDHO produces a description of the liquid that is almost as good as that obtained from an empirical model, TIP5P, that was fitted precisely to reproduce the experimental data of the liquid under ambient conditions. The MCDHO model slightly overestimates the density and the structure, and underestimates the vaporization enthalpy.

Two types of systems were used to show that MCDHO performs better than empirical models in describing water under conditions other than ambient: hexamers and ice Ih. We found that empirical models do produce various different conformations with energy differences similar to those obtained from *ab initio* calculations. Three-site models, though, were unable to yield the prism configuration. In all cases, the models produced hexamers more closely packed than their corresponding optimal dimers. Following the same trend, the structures of ice Ih predicted by the empirical models were all denser than that predicted with MCDHO, and this latter produces an overestimation of less than 1% on the experimentally determined value.

We further tested the effects of intramolecular flexibility and polarizability on the description of the energetics and structure of ice Ih, by using various versions of the MCDHO model with rigid constraints on the geometry and on the position of the shell, to fix the dipole moment at specified values. In agreement with a study of the liquid,[62] we found that a rigid, nonpolarizable model with the average ice molecular geometry and dipole, reproduces the results of the flexible and polarizable model. On the other hand, the description of the solid was modified when the geometry and the dipole were set at the liquid phase values, the larger difference produced by the lack of polarizability.

VII. CAVEATS AND CONCLUSIONS

Despite the large effort devoted to design transferable water models, such attempts were only recently able to correctly describe the various phases under different thermodynamical conditions.

Our results with the MCDHO model lead us to conclude that to achieve this goal, both polarizability and intramolecular flexibility have to be taken into account, and the intermolecular parameters should be fitted to the simplest pair interactions. As a consequence, numerical simulations with truly transferable models require an adequate handling of the various effects that are parametrized away in empirical effective potentials: long-range interactions, energetic costs of intramolecular deformations and polarization, and quantum effects due to intramolecular and intermolecular vibrations. This also affects classical simulations with quantum force fields.

In this and previous works, we have shown how to treat intramolecular flexibility in a thermodynamically correct way. However, the quantum effects of intramolecular vibrations have been neglected in our simulations. Work is in progress to include them within the Feynman–Hibbs approach.

One of the most stringent tests for flexible and polarizable models is how well they reproduce the phase diagram of water, and MC techniques can be used to study the liquid–vapor interface.[102] Work is also in progress in this direction, and preliminary results from histogram reweighting MC simulations yield a critical temperature of the MCDHO model that is in fairly good agreement with the experimental value, $T_c = 647$ K: between 550 and 570 K for MC-FF; between 650 and 670 K for MC-RC (ambient liquid water geometry), and between 620 and 640 K for MC-FC; all of them with a critical density close to the experimental value $\rho_c = 316\ \mathrm{kg\,m^{-3}}$. Though further analysis is needed, and will be published elsewhere, it is already clear that the method of flexible constraints is required for a correct classical simulation with a flexible model.

ACKNOWLEDGMENTS

This work was supported by NWO (The Netherlands), Project No. 433.078, by CONACyT (Mexico), Contract No. 020194, and by DGAPA-UNAM (Mexico) Project No. IN118602. H.S.-M. wants to thank Professor Alan Mark for his hospitality in his MD group at Rijksuniversiteit Groningen.

[1] B. Guillot, J. Mol. Liq. **101**, 219 (2002).
[2] H. J. C. Berendsen, J. P. M. Postma, W. F. van Gunsteren, and J. Hermans, in *Intermolecular Forces*, edited by B. Pullman (Reidel, Dordrecht, 1981), pp. 331–342.
[3] H. J. C. Berendsen, J. R. Grigera, and T. P. Straatsma, J. Phys. Chem. **91**, 6269 (1987).
[4] W. L. Jorgensen, J. Chandrasekhar, J. D. Madura, R. W. Impey, and M. L. Klein, J. Chem. Phys. **79**, 926 (1983).
[5] A. Glättli, X. Daura, and W. F. van Gunsteren, J. Chem. Phys. **116**, 9811 (2002).
[6] M. W. Mahoney and W. L. Jorgensen, J. Chem. Phys. **112**, 8910 (2000).
[7] K. Laasonen, M. Sprik, M. Parrinello, and R. Car, J. Chem. Phys. **99**, 9080 (1993).
[8] P. Silvestrelli and M. Parrinello, J. Chem. Phys. **111**, 3572 (1999).
[9] H. L. Lemberg and F. H. Stillinger, J. Chem. Phys. **62**, 1677 (1975).
[10] A. Rahman, F. H. Stillinger, and H. L. Lemberg, J. Chem. Phys. **63**, 5223 (1975).
[11] F. H. Stillinger and A. Rahman, J. Chem. Phys. **68**, 666 (1978).
[12] I. Benjamin, J. Chem. Phys. **95**, 3698 (1991).
[13] G. Corongiu, Int. J. Quantum Chem. **42**, 1209 (1992).
[14] S.-B. Zhu and G. W. Robinson, J. Chem. Phys. **97**, 4336 (1992).
[15] D. M. Ferguson, J. Comput. Chem. **16**, 501 (1995).
[16] I. G. Tironi, R. M. Brunne, and W. F. van Gunsteren, Chem. Phys. Lett. **250**, 19 (1996).

[17] R. P. Feynman and A. R. Hibbs, *Quantum Mechanics and Path Integrals* (McGraw–Hill, New York, 1965).
[18] M. Parrinello and A. Rahman, J. Chem. Phys. **80**, 860 (1984).
[19] J. Cao and G. A. Voth, J. Chem. Phys. **99**, 10070 (1993).
[20] J. Cao and G. A. Voth, J. Chem. Phys. **100**, 5106 (1994).
[21] J. Cao and G. A. Voth, J. Chem. Phys. **101**, 6157 (1994).
[22] J. Cao and G. A. Voth, J. Chem. Phys. **101**, 6168 (1994).
[23] R. A. Kuharski and P. J. Rossky, Chem. Phys. Lett. **103**, 357 (1984).
[24] R. A. Kuharski and P. J. Rossky, J. Chem. Phys. **82**, 5164 (1985).
[25] G. S. D. Buono, P. J. Rossky, and J. Schnitker, J. Chem. Phys. **95**, 3728 (1991).
[26] S. R. Billeter, P. M. King, and W. F. van Gunsteren, J. Chem. Phys. **100**, 6692 (1994).
[27] J. Lobaugh and G. A. Voth, J. Chem. Phys. **106**, 2400 (1997).
[28] H. A. Stern and B. J. Berne, J. Chem. Phys. **115**, 7622 (2001).
[29] B. Guillot and Y. Guissani, J. Chem. Phys. **108**, 10162 (1998).
[30] S. Reich, Physica D **89**, 28 (1995).
[31] J. Zhou, S. Reich, and B. R. Brooks, J. Chem. Phys. **112**, 7919 (2000).
[32] B. Hess, H. Saint-Martin, and H. J. C. Berendsen, J. Chem. Phys. **116**, 9602 (2002).
[33] H. Saint-Martin, J. Hernández-Cobos, M. I. Bernal-Uruchurtu, I. Ortega-Blake, and H. J. C. Berendsen, J. Chem. Phys. **113**, 10899 (2000).
[34] M. P. Allen and D. J. Tildesley, *Computer Simulations of Liquids* (Oxford Science Publications, Oxford, 1987).
[35] D. Frenkel and B. Smit, *Understanding Molecular Simulations: From Algorithms to Applications* (Academic, New York, 1996).
[36] W. L. Jorgensen and C. Jenson, J. Comput. Chem. **19**, 1179 (1998).
[37] H. C. Andersen, J. Chem. Phys. **72**, 2384 (1980).
[38] J. B. Sturgeon and B. B. Laird, J. Chem. Phys. **112**, 3474 (2000).
[39] H. J. C. Berendsen, J. P. M. Postma, W. F. van Gunsteren, A. DiNola, and J. R. Haak, J. Chem. Phys. **81**, 3684 (1984).
[40] N. Metropolis, A. W. Rosenbluth, M. N. Rosenbluth, A. H. Teller, and E. Teller, J. Chem. Phys. **21**, 1087 (1953).
[41] W. K. Hastings, Biometrika **57**, 92 (1970).
[42] G. S. Fishman, in *Monte Carlo. Concepts, Algorithms and Applications*, Springer Series on Operations Research (Springer, New York, 1996), Chap. 5.
[43] M. G. Martin, B. Chen, and J. I. Siepmann, J. Chem. Phys. **108**, 3383 (1998).
[44] V. I. Manousiothakis and M. W. Deem, J. Chem. Phys. **110**, 2753 (1999).
[45] M. Medeiros and M. E. Costas, J. Chem. Phys. **107**, 2012 (1997).
[46] H. Saint-Martin, C. Medina-Llanos, and I. Ortega-Blake, J. Chem. Phys. **93**, 6448 (1990).
[47] M. Předota, P. T. Cummings, and A. A. Chialvo, Mol. Phys. **99**, 349 (2001).
[48] E. M. Yezdimer and P. T. Cummings, Mol. Phys. **97**, 993 (1999).
[49] S. W. Rick, S. J. Stuart, and B. J. Berne, J. Chem. Phys. **101**, 6141 (1994).
[50] B. Chen, J. J. Potoff, and J. I. Siepmann, J. Phys. Chem. B **104**, 2378 (2000).
[51] M. Předota, P. T. Cummings, and A. A. Chialvo, Mol. Phys. **100**, 2703 (2002).
[52] A. A. Chialvo and P. T. Cummings, J. Chem. Phys. **105**, 8274 (1996).
[53] H. Flyvbjerg and H. G. Petersen, J. Chem. Phys. **91**, 461 (1989).
[54] P. P. Ewald, Ann. Phys. (N.Y.) **64**, 253 (1921).
[55] S. W. de Leeuw, J. W. Perram, and E. R. Smith, Proc. R. Soc. London, Ser. A **373**, 27 (1980).
[56] N. Karasawa and W. A. Goddard III, J. Phys. Chem. **93**, 7320 (1989).
[57] T. Darden, D. York, and L. Pedersen, J. Chem. Phys. **98**, 10089 (1993).
[58] B. A. Luty, M. E. Davies, I. G. Tironi, and W. F. van Gunsteren, Mol. Simul. **14**, 11 (1994).
[59] B. A. Luty, I. G. Tironi, and W. F. van Gunsteren, J. Chem. Phys. **103**, 3014 (1995).
[60] B. A. Luty and W. F. van Gunsteren, J. Phys. Chem. **100**, 2581 (1996).
[61] M. Carrillo-Tripp, H. Saint-Martin, and I. Ortega-Blake, J. Chem. Phys. **118**, 7062 (2003).
[62] J. Hernández, H. Saint-Martin, and I. Ortega-Blake (unpublished).
[63] A. K. Soper, Chem. Phys. **258**, 121 (2000).
[64] V. Buch, P. Sandler, and J. Sadlej, J. Phys. Chem. B **102**, 8641 (1998); the starting configuration of ice Ih was kindly provided by Professor Victoria Buch.
[65] E. Whalley, J. Chem. Phys. **81**, 4087 (1984).
[66] J. Kim and K. S. Kim, J. Chem. Phys. **109**, 5886 (1998).
[67] J. A. Niesse and H. R. Mayne, J. Comput. Chem. **18**, 1233 (1997).
[68] D. J. Wales and M. P. Hodges, Chem. Phys. Lett. **286**, 65 (1998).
[69] F. N. Keutsch and R. J. Saykally, Proc. Natl. Acad. Sci. U.S.A. **98**, 10533 (2001).
[70] S. S. Xantheas, C. J. Burnham, and R. J. Harrison, J. Chem. Phys. **116**, 1493 (2002).
[71] D. B. Chesnut, J. Phys. Chem. A **106**, 6876 (2002).
[72] K. Röttger, A. Endriss, J. Ihringer, S. Doyle, and W. F. Kuhs, Acta Crystallogr., Sect. B: Struct. Sci. **B50**, 644 (1994).
[73] J. Brodholt, M. Sampoli, and R. Vallauri, Mol. Phys. **85**, 81 (1995).
[74] O. A. Karim and A. D. J. Haymet, J. Chem. Phys. **89**, 6889 (1988).
[75] L. A. Báez and P. Clancy, Mol. Phys. **86**, 385 (1995).
[76] L. A. Báez and P. Clancy, J. Chem. Phys. **103**, 9744 (1995).
[77] S. W. Rick, J. Chem. Phys. **114**, 2276 (2001).
[78] S. C. Gay, E. J. Smith, and A. D. J. Haymet, J. Chem. Phys. **116**, 8876 (2002).
[79] C. J. Burnham and S. S. Xantheas, J. Chem. Phys. **116**, 1500 (2002).
[80] S. Dong, Y. Wang, and J. Li, Chem. Phys. **270**, 309 (2001).
[81] S.-H. Chen, K. Toukan, C.-K. Loong, D. L. Price, and J. Teixeira, Phys. Rev. Lett. **53**, 1360 (1984).
[82] F. Sciortino and G. Corongiu, J. Chem. Phys. **98**, 5694 (1993).
[83] K. Ichikawa, Y. Kameda, T. Yamaguchi, H. Wakita, and M. Misawa, Mol. Phys. **73**, 79 (1991).
[84] N. W. Moriarty and G. Karlström, J. Chem. Phys. **106**, 6470 (1997).
[85] T. M. Nymand and P. O. Åstrand, J. Phys. Chem. A **101**, 10039 (1997).
[86] C. J. Burnham and S. S. Xantheas, J. Chem. Phys. **116**, 5115 (2002).
[87] B. Hartke, Phys. Chem. Chem. Phys. **5**, 275 (2003).
[88] R. Chidambaran, Acta Crystallogr. **14**, 467 (1961).
[89] E. Whalley, Mol. Phys. **28**, 1105 (1974).
[90] W. F. Kuhs and M. S. Lehmann, J. Phys. (Paris) **48**, 3 (1987).
[91] V. M. Nield and R. W. Whitworth, J. Phys.: Condens. Matter **7**, 8259 (1995).
[92] Y. S. Badyal, M. L. Saboungi, D. L. Price, S. D. Shastri, D. R. Haeffner, and A. K. Soper, J. Chem. Phys. **112**, 9206 (2000).
[93] A. K. Soper, Mol. Phys. **99**, 1503 (2001).
[94] B. Guillot and Y. Guissani, J. Chem. Phys. **114**, 6720 (2001).
[95] H. Yu, T. Hansson, and W. F. van Gusnteren, J. Chem. Phys. **118**, 221 (2003).
[96] M. Alfredsson, J. P. Brodholt, K. Hermanson, and R. Vallauri, Mol. Phys. **94**, 873 (1998).
[97] H. Sato and F. Hirata, J. Chem. Phys. **111**, 8545 (1999).
[98] A. Morita, J. Comput. Chem. **23**, 1466 (2002).
[99] E. Whalley, J. Glaciol. **21**, 13 (1978).
[100] E. R. Batista, S. S. Xantheas, and H. Jónsson, J. Chem. Phys. **109**, 4546 (1998).
[101] E. R. Batista, S. S. Xantheas, and H. Jónsson, J. Chem. Phys. **111**, 6011 (1999).
[102] A. D. Mackie, J. Hernández-Cobos, and L. F. Vega, Mol. Simul. **24**, 63 (2000).
[103] G. S. Kell, J. Chem. Eng. Data **20**, 97 (1975).
[104] W. E. Thiessen and A. H. Narten, J. Chem. Phys. **77**, 2656 (1982).
[105] C. J. Burnham and S. S. Xantheas, J. Chem. Phys. **116**, 1479 (2002).